

Effect of inserting a non-metal C layer on the spin-orbit torque induced magnetization switching in Pt/Co/Ta structures with perpendicular magnetic anisotropy

Dong Li, Baoshan Cui, Tao Wang, Jijun Yun, Xiaobin Guo, Kai Wu, Yalu Zuo, Jianbo Wang, Dezheng Yang, and Li Xi

Citation: *Appl. Phys. Lett.* **110**, 132407 (2017);

View online: <https://doi.org/10.1063/1.4979468>

View Table of Contents: <http://aip.scitation.org/toc/apl/110/13>

Published by the [American Institute of Physics](#)

Articles you may be interested in

[Device-size dependence of field-free spin-orbit torque induced magnetization switching in antiferromagnet/ferromagnet structures](#)

Applied Physics Letters **110**, 092410 (2017); 10.1063/1.4977838

[Magnetization switching by spin-orbit torque in Pt with proximity-induced magnetic moment](#)

Journal of Applied Physics **121**, 123903 (2017); 10.1063/1.4978965

[Field-free spin-orbit torque switching of composite perpendicular CoFeB/Gd/CoFeB layers utilized for three-terminal magnetic tunnel junctions](#)

Applied Physics Letters **111**, 012402 (2017); 10.1063/1.4990994

[Giant interfacial perpendicular magnetic anisotropy in MgO/CoFe/capping layer structures](#)

Applied Physics Letters **110**, 072403 (2017); 10.1063/1.4976517

[Chiral magnetoresistance in Pt/Co/Pt zigzag wires](#)

Applied Physics Letters **110**, 122401 (2017); 10.1063/1.4979031

[Temperature dependence of spin-orbit effective fields in Pt/GdFeCo bilayers](#)

Applied Physics Letters **110**, 242405 (2017); 10.1063/1.4985436



Scilight

Sharp, quick summaries **illuminating**
the latest physics research

Sign up for **FREE!**

AIP
Publishing

Effect of inserting a non-metal C layer on the spin-orbit torque induced magnetization switching in Pt/Co/Ta structures with perpendicular magnetic anisotropy

Dong Li, Baoshan Cui, Tao Wang, Jijun Yun, Xiaobin Guo, Kai Wu, Yalu Zuo,^{a)} Jianbo Wang, Dezheng Yang, and Li Xi^{a)}

Key Laboratory for Magnetism and Magnetic Materials of Ministry of Education, Lanzhou University, Lanzhou 730000, People's Republic of China

(Received 24 December 2016; accepted 17 March 2017; published online 30 March 2017)

Magnetization switching via charge current induced spin-orbit torques (SOTs) in heavy metal/ferromagnetic metal/heavy metal heterostructures has become an important issue due to its potential applications in high stability and low energy dissipation spintronic devices. In this work, based on a Pt/Co/Ta structure with perpendicular magnetic anisotropy (PMA), we report the effect of inserting a non-metal C interlayer between Co and Ta on the current-induced magnetization switching. A series of measurements based on the extraordinary Hall effect were carried out to investigate the difference of the anisotropy field, switching field, and damping-like and field-like SOT-induced effective fields as well as the current-induced spin Hall effect (SHE) torque after C decoration. The results show that PMA can be reduced by C decoration and the ratio of the effective SHE torque per unit current density and anisotropy field plays an essential role in the switching efficiency. In addition, the obtained switching current density has a quite low value around the order of 10^6 A/cm². Our study could provide a way for achieving the low switching current density by manipulating PMA in SOT-based spintronic devices through interface decoration. Published by AIP Publishing. [<http://dx.doi.org/10.1063/1.4979468>]

Current-induced spin orbit torques (SOTs) in heavy metals (HMs) with strong spin-orbit coupling (SOC) have become an intriguing issue in recent years due to their essential role in highly efficient magnetization switching^{1–6} and fast domain wall motion.^{7–12} The SOTs from the bulk spin Hall effect (SHE)^{4,9,10} and/or the interfacial Rashba effect^{1,13–15} which can generate the damping-like (DL) and field-like (FL) effective fields have been studied to manipulate the magnetization in ultra-thin ferromagnetic (FM) layers with perpendicular magnetic anisotropy (PMA) in different structures and systems. In particular, the HM/FM/oxide system including Ta/CoFeB/MgO,^{16–19} W/Co₂FeAl/MgO,²⁰ W/CoFeB/MgO,²¹ and Hf/CoFeB/MgO,²² and the HM/FM/HM system with two HMs which show opposite signs of spin Hall angle (θ_{SH}) including Pt/Co/Ta,²³ Pt/Co-Ni/W,²⁴ and Pt/Co/Gd²⁵ have been investigated to enhance the effective SOTs and reduce the switching current density (J_c). Most of the above investigations mainly focus on choosing HMs with large θ_{SH} or the structures with large effective θ_{SH} to improve the SOT's efficiency. Recent reports^{26,27} on manipulating the SOTs and even the magnetic anisotropy through the interfacial non-magnetic metal Cu decoration have attracted attention. In the SHE picture, J_c is not only related to the strength of the effective SHE torque (τ_{ST}^0), but also associated with the perpendicular magnetic anisotropy field (H_{an}^0).⁴ Both the enhanced τ_{ST}^0 and reduced H_{an}^0 can reduce J_c .

Graphite (C) composed of light-weight element carbon with weak SOC has a weak spin scattering and long spin relaxation time.²⁸ It makes C a viable candidate for

spin-transport materials.^{29,30} In this work, we investigate the effect of inserting a non-metal C interlayer between Co and Ta on the current-induced magnetization switching (CIMS) in Pt/Co/Ta with PMA. The changes of the effective SHE torque per unit current density ($\beta_{ST}^0 = \tau_{ST}^0/J_e$, J_e is the charge current density) and H_{an}^0 reveal that the ratio (β_{ST}^0/H_{an}^0) plays a key role in the switching efficiency. A relatively low J_c threshold can be obtained by means of C decoration through reducing PMA. Furthermore, we demonstrate the CIMS for the current density of the order of 10^6 A/cm² in Ta/Pt/Co/Ta and Ta/Pt/Co/C/Ta.

Two film stacks Ta(3)/Pt(5)/Co(0.6)/Ta(5) and Ta(3)/Pt(5)/Co(0.6)/C(2)/Ta(5) (thickness in nm) were deposited on corning glass substrates at room temperature (RT) by direct current (DC) magnetron sputtering with a base pressure below 4.0×10^{-5} Pa. Among them, the bottom 3 nm Ta is used as the seed layer and the top Ta layer has an around 1.5 nm TaOx capping layer due to the air exposure.^{23,31} Afterwards, the stacks were patterned into 8.5 μ m wide Hall bars using standard lithography and Ar-ion milling techniques. The PMA was obtained by annealing the devices at 400 °C for 1 h with a base pressure 3.0×10^{-4} Pa for Ta/Pt/Co/C/Ta structures. The Hall resistances were measured using standard DC and AC analysis techniques. All the measurements were made at RT.

Fig. 1(a) schematically shows the device structure and measurement configuration. Figs. 1(c) and 1(d) illustrate the Hall resistance (R_{Hall}) as a function of H_z under +1 mA (the current direction is shown in Fig. 1(a)) in Ta/Pt/Co/Ta and Ta/Pt/Co/C/Ta, respectively. The square shaped loops confirm the presence of PMA. Moreover, R_{Hall} is proportional to the perpendicular component of magnetization (M_z) of the

^{a)} Authors to whom correspondence should be addressed. Electronic addresses: zuoyl@lzu.edu.cn and xili@lzu.edu.cn

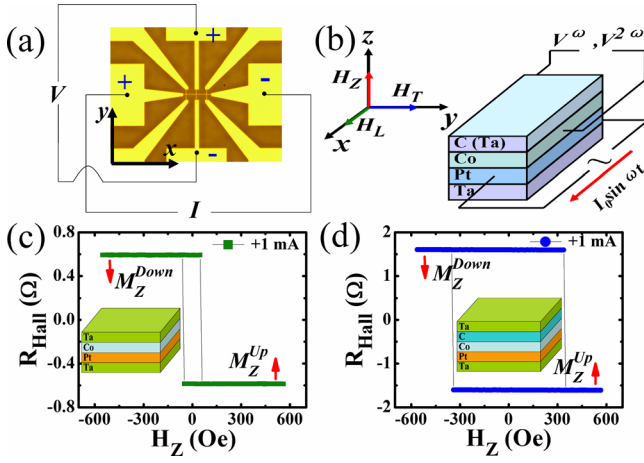


FIG. 1. (a) Optical image of the patterned Hall bar and the DC experiment configuration. (b) Schematic diagram of the Pt/Co/(C)/Ta and experimental setup of the SOT-induced damping-like and field-like effective field measurement. Dependence of R_{Hall} on H_z was measured at +1 mA in Ta/Pt/Co/Ta (c) and Ta/Pt/Co/C/Ta (d) stacks.

Co layer, which can thus be used to identify the direction of magnetization with M_Z^{up} (M_Z^{down}) corresponding to $R_{Hall} < 0$ ($R_{Hall} > 0$) as labeled by red arrows.

The switching field (H_{sw}) extracted from the R_{Hall} - H_z loops with different currents (I) is shown in Fig. 2(a). It can be seen that H_{sw} decreases remarkably as the current increases for Ta/Pt/Co/C/Ta, while the H_{sw} changes little for Ta/Pt/Co/Ta. It may be ascribed to the decreased PMA in Ta/Pt/Co/C/Ta due to C decoration, which makes H_{sw} readily affected by the increased current-induced torque related to the SHE when the current increases (Joule heating effect can be negligible, which will be discussed below). Furthermore, in Fig. 2(b), we summarize H_{sw} against the angle θ obtained from the angle dependent R_{Hall} - H_z loops which are measured at $I = 0.5$ mA to reduce the spin Hall torque. From Fig. 2(b), one can see that the H_{sw} follows an inverse $\cos\theta$ curve shown in solid lines at small angles.^{32,33} This kind of relationship indicates that the magnetization reversal is dominated by depinning of domain walls in the large anisotropic systems

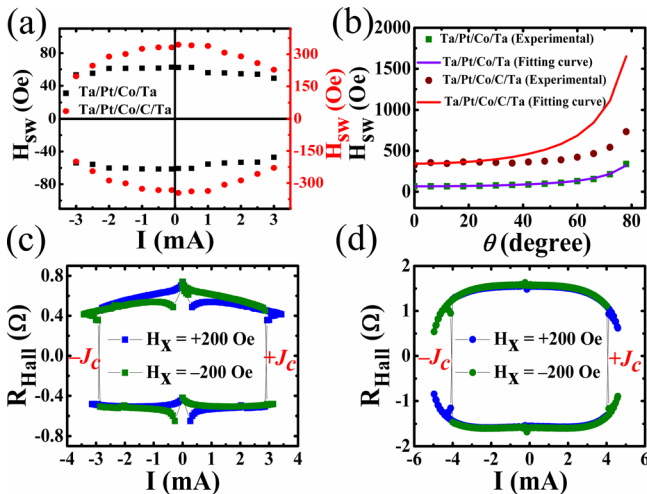


FIG. 2. Switching field as a function of current I (a) and angle θ (b), showing the effect of adding a C layer. CIMS loops in Ta/Pt/Co/Ta (c) and Ta/Pt/Co/C/Ta (d) with an assistance of the in-plane constant field H_x of ± 200 Oe. θ is the angle between the external magnetic field (H_{ext}) and z axis.

($H_{sw} \ll H_{an}^0$)³⁴ when the magnetic field deviates from out-of-plane in a small angle range. However, for Ta/Pt/Co/C/Ta, the H_{sw} remarkably deviates from the $1/\cos\theta$ dependence in the large angle ranges in comparison with Ta/Pt/Co/Ta, indicating the reduced anisotropy field in Ta/Pt/Co/C/Ta. It can be explained by that the coherent rotation process plays a dominant role in the magnetization reversal at large angles, which reduces the H_{sw} in total.³² Thus, we conclude that PMA is reduced by C decoration. In addition, the increased H_{sw} for the device with a C interlayer may be explained by a relatively large pinning field existing due to some interdiffusion between the Co and C layers. Figs. 2(c) and 2(d) show the CIMS curves under in-plane assisted magnetic field $H_x = \pm 200$ Oe along the current direction for Ta/Pt/Co/Ta and Ta/Pt/Co/C/Ta, respectively. Due to M_Z^{up} (M_Z^{down}) corresponding to $R_{Hall} < 0$ ($R_{Hall} > 0$) in our experiment, the direction of current and H_x determines the polarity of the switching, which is consistent with the model of the SHE switching.⁴ In addition, the J_c for the assisted field $H_x = \pm 200$ Oe is around 2.82×10^6 and 3.39×10^6 A/cm² for Ta/Pt/Co/Ta and Ta/Pt/Co/C/Ta, respectively, if we assume the uniform current flows across metallic layers and the C interlayer. Although the approximate and relatively low J_c of the order of 10^6 A/cm² is obtained for the two devices, J_c is not further reduced due to the reduced PMA when inserting a C layer. It can be ascribed to the decreased current-induced SHE torque for Ta/Pt/Co/C/Ta. The further investigations will be shown in the next part.

Next, the harmonic Hall voltage measurement technique was used to quantify the current-induced SOT effective fields. The measurement diagram is depicted in Fig. 1(b). A sinusoidal current with a frequency of 133 Hz along x axis was passed through the Hall bars and the first (V^ω) and second ($V^{2\omega}$) harmonic voltages along y axis were collected using the Analog-Digital/Digital-Analog card by the frequency-spectra analysis. H_{ext} was applied along the x (longitudinal-field H_L) and y (transverse-field H_T) directions to obtain the longitudinal damping-like effective field (H^{DL}) and the transverse field-like effective field (H^{FL}), which is, respectively, induced by the damping-like and field-like SOTs using the equations¹⁷

$$H^{DL(FL)} = -2 \frac{\partial V^{2\omega}}{\partial H_{L(T)}} / \frac{\partial^2 V^\omega}{\partial H_{L(T)}^2}. \quad (1)$$

Figs. 3(a)–3(d) show V^ω as a function of H_L and H_T for Ta/Pt/Co/Ta and Ta/Pt/Co/C/Ta, respectively. The insets of each figure represent $V^{2\omega}$ as a function of H_L and H_T . In addition, in order to obtain H^{DL} and H^{FL} using Eq. (1), the first and second harmonic curves were, respectively, fitted using the quadratic and linear fitting function.¹⁷ The calculated H^{DL} is plotted with respect to the amplitude (I_0) of the sinusoidal current for both devices in Figs. 4(a) and 4(c). The effective fields are linear with I_0 , indicating that the Joule heating and other non-linear effects can be negligible in our experiment.³⁵ H^{DL} per unit current density (β_{DL}) is found to be -3.98 ± 0.20 Oe/(10^6 A/cm²) (3.93 ± 0.12 Oe/(10^6 A/cm²)) for the “up” (“down”) magnetized states in Ta/Pt/Co/C/Ta and -8.11 ± 0.14 Oe/(10^6 A/cm²) (8.76 ± 0.12 Oe/(10^6 A/cm²)) for the “up” (“down”) magnetized states in Ta/Pt/Co/Ta. It is two times larger for Ta/Pt/

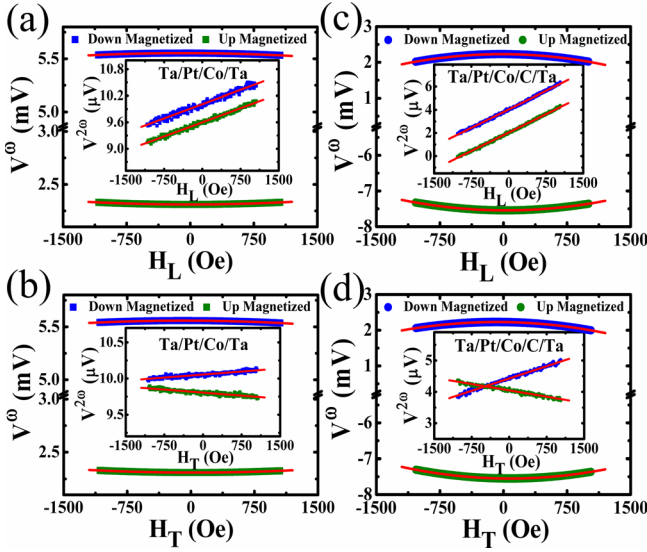


FIG. 3. (a)–(d) First harmonic voltages V^0 versus in-plane longitudinal H_L and transverse H_T swept magnetic fields. The inset in each figure shows the second harmonic voltage $V^{2\omega}$ as a function of H_L and H_T . The solid green and blue symbols correspond to “up” and “down” magnetized states, respectively. The red lines stand for the quadratic and linear fitting.

Co/Ta than that for Ta/Pt/Co/C/Ta, revealing that the β_{DL} is reduced after inserting a C layer.

Similarly, the calculated H^{FL} is displayed in Figs. 4(b) and 4(d). The dependence of H^{FL} on I_0 is also linear for the “up” and “down” magnetized states. H^{FL} per unit current density (β_{FL}) is found to be $0.99 \pm 0.06 \text{ Oe}/(10^6 \text{ A/cm}^2)$ ($1.09 \pm 0.06 \text{ Oe}/(10^6 \text{ A/cm}^2)$) for the “up” (“down”) magnetized states in Ta/Pt/Co/C/Ta and $1.13 \pm 0.03 \text{ Oe}/(10^6 \text{ A/cm}^2)$ ($1.03 \pm 0.02 \text{ Oe}/(10^6 \text{ A/cm}^2)$) for the “up” (“down”) magnetized states in Ta/Pt/Co/Ta. It is evident that the β_{FL} is almost equivalent, indicating that the J_c for both devices is determined by damping-like SOT and H_{an}^0 .

In order to quantitatively evaluate H_{an}^0 and τ_{ST}^0 and understand the relationship between J_c and them, we

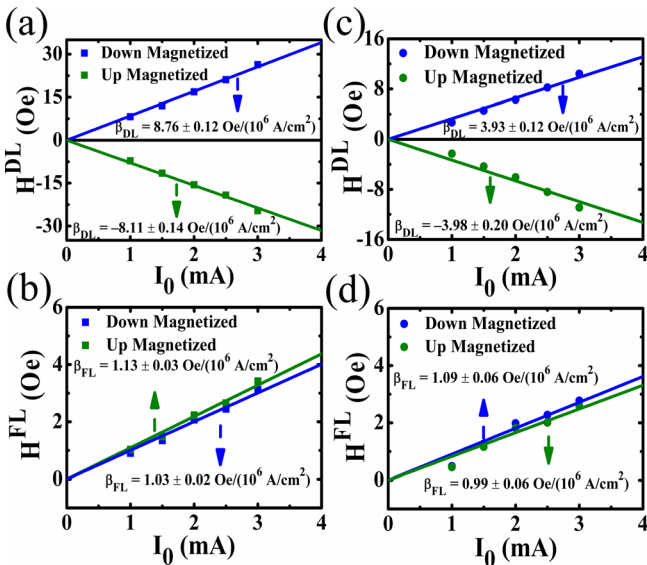


FIG. 4. (a)–(d) damping-like (field-like) SOT-induced effective field for Ta/Pt/Co/Ta (Ta/Pt/Co/C/Ta) against the amplitude of the sinusoidal current. The slope of the fitted curves gives $\beta_{DL, FL} = H^{DL, FL}/J_c$. The green and blue symbols represent “up” and “down” magnetized states, respectively.

measure R_{Hall} under a sweeping magnetic field H_{ext} to compare the difference of the R_{Hall} - H_{ext} curves under the same magnitude of positive and negative constant charge current. The schematic measurement diagram is shown in the inset of Fig. 5(a) and α is the angle between the magnetization \mathbf{M} and x axis, which is determined via measuring R_{Hall} . i.e., $\sin\alpha = R_{Hall}/R_0$. R_0 is the maximum Hall resistance when the magnetization \mathbf{M} is along the z axis. And δ is the angle between \mathbf{H}_{ext} and x axis in the x - z plane. Therefore, H_{an}^0 and τ_{ST}^0 can be quantitatively analyzed by the equilibrium equation⁴

$$\tau_{tot} = \tau_{ST}^0 + H_{ext} \sin(\alpha - \delta) - H_{an}^0 \sin\alpha \cos\alpha = 0, \quad (2)$$

where $\tau_{ST}^0 = \hbar J_s / 2eM_s t_{FM}$. Fig. 5(a) illustrates R_{Hall} ($=R_0 \sin\alpha$) as a function of H_{ext} within the x - z plane at an angle $\delta = 15^\circ$ to the x axis with $\pm 2 \text{ mA}$ DC for Ta/Pt/Co/C/Ta. For an arbitrary $R_0 \sin\alpha$, $H_+(\alpha)$ and $H_-(\alpha)$, respectively, corresponding to the positive and negative current can be obtained. Thus, from Eq. (2), one can obtain the equation

$$\tau_{ST}^0(+J_s) + H_+(\alpha) \sin(\alpha - \delta) - H_{an}^0 \sin\alpha \cos\alpha = 0, \quad (3)$$

$$\tau_{ST}^0(-J_s) + H_-(\alpha) \sin(\alpha - \delta) - H_{an}^0 \sin\alpha \cos\alpha = 0. \quad (4)$$

Using the combination of (3) and (4), one can obtain

$$[H_+(\alpha) - H_-(\alpha)] = 2\tau_{ST}^0 / \sin(\alpha - \delta), \quad (5)$$

$$[H_+(\alpha) + H_-(\alpha)] = 2H_{an}^0 \sin\alpha \cos\alpha / \sin(\alpha - \delta). \quad (6)$$

And then using Eqs. (5) and (6), one can fit the experimental data to calculate τ_{ST}^0 and H_{an}^0 . Fig. 5(b) shows the $[H_+(\alpha) - H_-(\alpha)]$ as a function of $1/\sin(\alpha - \delta)$ and Fig. 5(c) shows the $[H_+(\alpha) + H_-(\alpha)]$ against $\sin\alpha \cos\alpha / \sin(\alpha - \delta)$ for Ta/Pt/Co/C/Ta. The insets in Figs. 5(b) and 5(c) show the corresponding

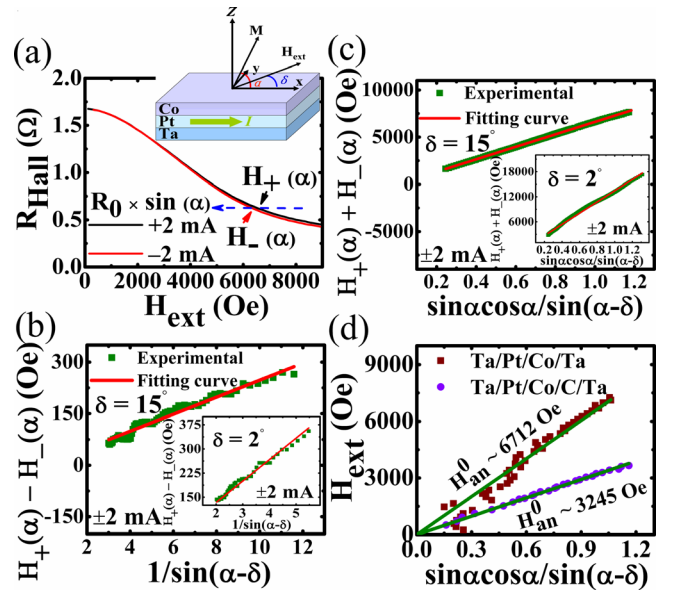


FIG. 5. (a) R_{Hall} as a function of H_{ext} with $\pm 2 \text{ mA}$ DC for Ta/Pt/Co/C/Ta. The inset shows the schematic measurement diagram. (b) The linear fitting between $[H_+(\alpha) - H_-(\alpha)]$ and $1/\sin(\alpha - \delta)$ based on Eq. (5) and the inset is for Ta/Pt/Co/Ta. (c) The linear fitting between $[H_+(\alpha) + H_-(\alpha)]$ and $\sin\alpha \cos\alpha / \sin(\alpha - \delta)$ based on Eq. (6) and the inset is for Ta/Pt/Co/Ta. (d) The H_{ext} versus $\sin\alpha \cos\alpha / \sin(\alpha - \delta)$ with a linear fitting based on Eq. (8).

results for Ta/Pt/Co/Ta. The obtained τ_{ST}^0 is 12.38 ± 0.21 Oe and 33.37 ± 0.38 Oe under the ± 2 mA current corresponding to 7.42 ± 0.13 Oe/(10^6 A/cm²) and 17.16 ± 0.20 Oe/(10^6 A/cm²) for Ta/Pt/Co/C/Ta and Ta/Pt/Co/Ta, respectively. It reveals that the β_{ST}^0 for Ta/Pt/Co/Ta is also about two times larger than that for Ta/Pt/Co/C/Ta. It is worth to note that both β_{ST}^0 for Ta/Pt/Co/C/Ta and Ta/Pt/Co/Ta are about two times larger than the β_{DL} discussed above, which is due to not taking the planar Hall effect (PHE) correction into consideration in the harmonic Hall voltages measurements.²³ Meanwhile, according to the formula³⁶

$$\theta_{SH} = J_s/J_e = (2|e|M_s t_{FM}/\hbar)(\tau_{ST}^0/J_e), \quad (7)$$

where e is the elementary charge, t_{FM} is the thickness of the ferromagnetic layer, \hbar is the reduced Planck constant, and cobalt saturation magnetization M_s is about 1.288×10^6 and 1.213×10^6 A/m for Ta/Pt/Co/C/Ta and Ta/Pt/Co/Ta, respectively, the calculated effective θ_{SH} is 0.379 ± 0.004 for Ta/Pt/Co/Ta. The value is also similar to that reported in the Pt/Co/Ta system.²³ However, it is 0.174 ± 0.003 for Ta/Pt/Co/C/Ta, which is ascribed to the decreased β_{ST}^0 as discussed above. From Fig. 5(c), the H_{an}^0 is 3308 ± 4 Oe and 6728 ± 27 Oe for Ta/Pt/Co/C/Ta and Ta/Pt/Co/Ta, respectively. By comparison, the anisotropy field decreases more than half when inserting a C interlayer between Co and Ta layers, which is in agreement with the qualitative discussion above. And then we also estimate H_{an}^0 using another method. When reducing the charge current close to zero, the Eq. (3) or (4) can be replaced by³⁶

$$H_{ext} = H_{an}^0 \sin \alpha \cos \alpha / \sin(\alpha - \delta). \quad (8)$$

Fig. 5(d) shows the fitting curves and results based on Eq. (8). The obtained H_{an}^0 is very similar to the values obtained using the first method. As a result, H_{an}^0 indeed has a dramatic decrease by C decoration.

Finally, the relationship between the J_c and H_{an}^0 as well as β_{ST}^0 is quantitatively elaborated. We use β_{ST}^0/H_{an}^0 to determine J_c . If β_{ST}^0/H_{an}^0 is large, J_c becomes low, and vice versa. Thus, low J_c can be obtained if enhancing β_{ST}^0 or reducing adequately H_{an}^0 . In our experiment, β_{ST}^0/H_{an}^0 is found to be $2.24 \pm 0.04/(10^9$ A/cm²) for Ta/Pt/Co/C/Ta and $2.55 \pm 0.03/(10^9$ A/cm²) for Ta/Pt/Co/Ta. That is, the value of β_{ST}^0/H_{an}^0 is not raised while inserting a C layer. Therefore, the J_c is also not decreased compared to that for Ta/Pt/Co/Ta. It can be understood by the fact that although the H_{an}^0 is dropped by C decoration, the β_{ST}^0 is also reduced. One possible reason for the reduced effective torque while inserting a C layer is that the C layer in the experiment was deposited by sputtering, which could lead to form some defects in the C layer. Therefore, the spin current resulting from the top Ta layer may be partly scattered when it flows through the C interlayer. And another possibility is that some interdiffusion and chemical reaction from the interface between Co and C as well as the interface between C and Ta may also increase the spin flipping probability.³⁷ Moreover, the large pinning field in Ta/Pt/Co/C/Ta due to some interdiffusion between Co and C is also responsible for the not reduced J_c . As a consequence, the low J_c can be achieved by reducing the

PMA through C decoration on the basis of enhancing and improving the quality of the C layer and the interfacial environment.

In summary, we have investigated the effect of inserting a C interlayer between Co and Ta on the anisotropy field, spin orbit torques, and the associated effective fields in Pt/Co/Ta structures with perpendicular magnetic anisotropy. The obtained magnetization switching current density is in the order of 10^6 A/cm² in both Ta/Pt/Co/Ta and Ta/Pt/Co/C/Ta devices. Both the anisotropy field and the effective SHE torque per unit current density are reduced by nearly a half by C decoration due to the change of interfacial magnetic anisotropy and the formation of defects during C sputtering. However, the switching current density changes a little since the ratio between the effective SHE torque per unit current density and anisotropy field plays an important role in the current-induced magnetization switching. Thus, further decreasing the switching current density could be realized by C decoration with a high quality interface for free spin current transport. Our study could provide a way for achieving the low switching current density by manipulating the perpendicular magnetic anisotropy through the non-metal C decoration in SOT-based spintronic devices.

This work was supported by the Program for Changjiang Scholars and Innovative Research Team in University PCSIRT (No. IRT16R35), the National Natural Science Foundation of China (No. 51671098), the Fundamental Research Funds for Central Universities (Izujbky-2015-122), and the Natural Science Foundation of Gansu Province (No. 145RJZA154).

- ¹I. M. Miron, K. Garello, G. Gaudin, P. J. Zermatten, M. V. Costache, S. Auffret, S. Bandiera, B. Rodmacq, A. Schuhl, and P. Gambardella, *Nature* **476**, 189 (2011).
- ²C. O. Avci, K. Garello, I. M. Miron, G. Gaudin, S. Auffret, O. Boulle, and P. Gambardella, *Appl. Phys. Lett.* **100**, 212404 (2012).
- ³L. Liu, C. F. Pai, Y. Li, H. W. Tseng, D. C. Ralph, and R. A. Buhrman, *Science* **336**, 555 (2012).
- ⁴L. Liu, Q. J. Lee, T. J. Gudmundsen, D. C. Ralph, and R. A. Buhrman, *Phys. Rev. Lett.* **109**, 096602 (2012).
- ⁵J. Torrejon, F. Garcia-Sanchez, T. Taniguchi, J. Sinha, S. Mitani, J. V. Kim, and M. Hayashi, *Phys. Rev. B* **91**, 214434 (2015).
- ⁶M. H. Nguyen, C. F. Pai, K. X. Nguyen, D. A. Muller, D. C. Ralph, and R. A. Buhrman, *Appl. Phys. Lett.* **106**, 222402 (2015).
- ⁷T. A. Moore, I. M. Miron, G. Gaudin, G. Serret, S. Auffret, B. Rodmacq, A. Schuhl, S. Pizzini, J. Vogel, and M. Bonfim, *Appl. Phys. Lett.* **93**, 262504 (2008).
- ⁸D. Chiba, M. Kawaguchi, S. Fukami, N. Ishiwata, K. Shimamura, K. Kobayashi, and T. Ono, *Nat. Commun.* **3**, 888 (2012).
- ⁹S. Emori, U. Bauer, S. M. Ahn, E. Martinez, and G. S. D. Beach, *Nat. Mater.* **12**, 611 (2013).
- ¹⁰P. P. J. Haazen, E. Murè, J. H. Franken, R. Lavrijsen, H. J. M. Swagten, and B. Koopmans, *Nat. Mater.* **12**, 299 (2013).
- ¹¹K. S. Ryu, L. Thomas, S. H. Yang, and S. Parkin, *Nat. Nanotechnol.* **8**, 527 (2013).
- ¹²S. H. Yang, K. S. Ryu, and S. Parkin, *Nat. Nanotechnol.* **10**, 221 (2015).
- ¹³I. M. Miron, G. Gaudin, S. Auffret, B. Rodmacq, A. Schuhl, S. Pizzini, J. Vogel, and P. Gambardella, *Nat. Mater.* **9**, 230 (2010).
- ¹⁴K. W. Kim, S. M. Seo, J. Ryu, K. J. Lee, and H. W. Lee, *Phys. Rev. B* **85**, 180404 (2012).
- ¹⁵X. Qiu, K. Narayanapillai, Y. Wu, P. Deorani, D. H. Yang, W. S. Noh, J. H. Park, K. J. Lee, H. W. Lee, and H. Yang, *Nat. Nanotechnol.* **10**, 333 (2015).
- ¹⁶T. Suzuki, S. Fukami, N. Ishiwata, M. Yamanouchi, S. Ikeda, N. Kasai, and H. Ohno, *Appl. Phys. Lett.* **98**, 142505 (2011).

- ¹⁷J. Kim, J. Sinha, M. Hayashi, M. Yamanouchi, S. Fukami, T. Suzuki, S. Mitani, and H. Ohno, *Nat. Mater.* **12**, 240 (2013).
- ¹⁸G. Yu, P. Upadhyaya, K. L. Wong, W. Jiang, J. G. Alzate, J. Tang, P. K. Amiri, and K. L. Wang, *Phys. Rev. B* **89**, 104421 (2014).
- ¹⁹C. O. Avci, K. Garello, C. Nistor, S. Godey, B. Ballesteros, A. Mugarza, A. Barla, M. Valvidares, E. Pellegrin, A. Ghosh, I. M. Miron, O. Boulle, S. Auffret, G. Gaudin, and P. Gambardella, *Phys. Rev. B* **89**, 214419 (2014).
- ²⁰M. S. Gabor, T. Petrisor, Jr., R. B. Mos, A. Mesaros, M. Nasui, M. Belmeguenai, F. Zighem, and C. Tiusan, *J. Phys. D: Appl. Phys.* **49**, 365003 (2016).
- ²¹C. Zhang, S. Fukami, K. Watanabe, A. Ohkawara, S. D. Gupta, H. Sato, F. Matsukura, and H. Ohno, *Appl. Phys. Lett.* **109**, 192405 (2016).
- ²²R. Ramaswamy, X. Qiu, T. Dutta, S. D. Pollard, and H. Yang, *Appl. Phys. Lett.* **108**, 202406 (2016).
- ²³S. Woo, M. Mann, A. J. Tan, L. Caretta, and G. S. D. Beach, *Appl. Phys. Lett.* **105**, 212404 (2014).
- ²⁴J. W. Yu, X. P. Qiu, W. Legrand, and H. Yang, *Appl. Phys. Lett.* **109**, 042403 (2016).
- ²⁵K. Ueda, C. F. Pai, A. J. Tan, M. Mann, and G. S. D. Beach, *Appl. Phys. Lett.* **108**, 232405 (2016).
- ²⁶W. F. Zhang, W. Han, X. Jiang, S. H. Yang, and S. S. P. Parkin, *Nat. Phys.* **11**, 496 (2015).
- ²⁷T. X. Nan, S. Emori, C. T. Boone, X. J. Wang, T. M. Oxholm, J. G. Jones, B. M. Howe, G. J. Brown, and N. X. Sun, *Phys. Rev. B* **91**, 214416 (2015).
- ²⁸S. Sanvito and A. R. Rocha, *J. Comput. Theor. Nanosci.* **3**, 624 (2006).
- ²⁹Z. H. Xiong, D. Wu, Z. V. Vardeny, and J. Shi, *Nature* **427**, 821 (2004).
- ³⁰V. A. Dediu, L. E. Hueso, I. Bergenti, and C. Taliani, *Nat. Mater.* **8**, 707 (2009).
- ³¹M. Akyol, J. G. Alzate, G. Q. Yu, P. Upadhyaya, K. L. Wong, A. Ekicibil, P. K. Amiri, and K. L. Wang, *Appl. Phys. Lett.* **106**, 032406 (2015).
- ³²O. J. Lee, L. Q. Liu, C. F. Pai, Y. Li, H. W. Tseng, P. G. Gowtham, J. P. Park, D. C. Ralph, and R. A. Buhrman, *Phys. Rev. B* **89**, 024418 (2014).
- ³³F. Schumacher, *J. Appl. Phys.* **70**, 3184 (1991).
- ³⁴A. Singh, V. Neu, S. Fähler, K. Nenkov, L. Schultz, and B. Holzapfel, *Phys. Rev. B* **77**, 104443 (2008).
- ³⁵D. Wu, G. Q. Yu, C.-T. Chen, S. A. Razavi, Q. M. Shao, X. Li, B. C. Zhao, K. L. Wong, C. L. He, Z. Z. Zhang, P. K. Amiri, and K. L. Wang, *Appl. Phys. Lett.* **109**, 222401 (2016).
- ³⁶Q. Hao and G. Xiao, *Phys. Rev. B* **91**, 224413 (2015).
- ³⁷D. Li, X. B. Guo, K. Wu, B. S. Cui, Y. L. Zuo, J. B. Wang, and L. Xi, *Appl. Surf. Sci.* **357**, 1040 (2015).